Proceedings of the 2019 IEEE/SICE
International Symposium on System Integration
Paris, France, January 14-16, 2019

Safety Aura Visualization for Variable Impedance Actuated Robots

Zhanat Makhataeva, Altay Zhakatayev, Huseyin Atakan Varol, *Senior Member, IEEE*

***Abstract*— This paper presents an augmented reality-based method to increase human cognitive awareness of the danger/safety in the workspace of a variable impedance actuated (VIA) robot. Specifically, the "safety aura" around the robot was created using a safety/index defined for each point of the workspace. The safety-index is a composite metric incorporating the measurements of the distance from a point in the workspace to the VIA robot and the corresponding velocity during its motion. The safety aura is task-specific and is able to represent the safety levels in the workspace of the robot as it follows different trajectories. We developed a robot simulator which allows the visualization of the robot's motion and assessment of the corresponding safety aura in 3D space. The generated safety aura was overlaid into mixed reality using Unity 3D platform together with Vuforia and web camera. Simulation results demonstrated the ability of the safety metric based on distance and velocity measurements to qualitatively assess the amount of danger. Our method has the potential to make the physical human robot interaction safer.**

I. Introduction

Traditional position-controlled robots outperform humans in terms of motion speed, power, position accuracy and repeatability. Due to these advantages utilization of these robots in industry is steadily growing. According to the report of the International Federation of Robots, in the year 2016 alone robot sales worldwide have increased by 16%, and came close to 300,000 [1]. The same report highlighted that the number of industrial robot sales will exceed 500,000 units by 2020. The robot utilization has become popular in automotive and electrical/electronics industries. The trend toward automation drives the demand for robots upward.

Physical human-robot interaction (pHRI) has become an important area in the robotics research community. However, traditional rigid robots are not appropriate for this task due to multiple reasons. Firstly, rigid robots do not have agility and dexterity comparable with the level of humans and animals. Secondly, safety of a human and integrity of a robot are at risk during operation in dynamic and unknown environments. The existing solution to the latter issue is to completely isolate the workspace of rigid robots from human access during their operation. However, this "workcell" solution is ad-hoc, impractical, and inefficient.

This work was supported by the grant "Methods for Safe Human Robot Interaction with VIA Robots" from the Ministry of Education and Science of the Republic of Kazakhstan and by the Nazarbayev University Faculty Development Program grant "Hardware and Software Based Methods for Safe Human-Robot Interaction with Variable Impedance Robots".

Z. Makhataeva, A. Zhakatayev, and H. A. Varol are with the Dept. of Robotics and Mechatronics, Nazarbayev University, 53 Kabanbay Batyr Ave, Z05H0P9 Astana, Kazakhstan. Email: {zhanat.mahataeva,azhakatayev,ahvarol}@nu.edu.kz
Corresponding author: H. Atakan Varol.

From the perspective of robot design and control, two broad solutions addressing the safety are pursued by the robotics community. *Active compliance control* is based on incorporating force/torque sensors to joints, reducing the mass/inertia of the robot links, and utilization of clever control algorithms [2]–[4]. Even though this method somewhat alleviates the safety and agility problems of rigid robots, it does not resolve them fully. Due to very rapid motion of the robot or failure of a sensor and/or controller, active compliance still might result in injury in case of a collision. Therefore, *passive compliance control* was developed as an alternative solution to the safety problem. The main idea behind passive compliance is to replace rigid joints with variable impedance ones. This resulted in the so called *variable impedance actuated* (VIA) robots [5]. In effect, active compliance control is based on making mechanically rigid robot behave as a compliant robot, while passive compliance control is focused on designing and controlling mechanically compliant robots. A three degrees-of-freedom (DoF) variable impedance actuated robot with three actuators and three nonlinear elastic elements is shown in Fig. 1.

The core principle behind VIA robots is to adjust, depending on the task, the mechanical impedance of the robot joints. This is achieved through mechanical decoupling of the link inertia from the gear and the actuator inertia. In addition to safety, VIA robots have other advantages compared to the rigid robots, which are related to the energy efficiency and capability to adjust the systems' natural modes of oscillation. Over the years significant advances have been made in the control of VIA robots [6]–[8]. However, the research on how to convey information about VIA robot's state to a human operator is scarce.

Multiple danger-indexes and safety strategies were introduced for pHRI. Among many safety indexes used in the automotive industry, the most popular ones are the Head Injury Criteria (HIC) [9] and Gadd Severity Index (GSI) [10]. HIC whose effectiveness was validated on experiments involving automobile crash tests, cannot be considered as an effective measure of the danger in cases of human-robot collision [11]. This is due to high velocities involved in automobile crashes, while robots in general operate at much less velocities. As the workspaces of humans and robots transform to be more integrated, a solid understanding of the safe/danger zones by the human operator becomes essential for proper decision making [12]. Growing importance of pHRI increases the need for effective methods capable of ensuring the human safety.

One way to ensure safety during pHRI is to restrict the kinematic and dynamic properties of the robot motion

978-1-5386-3615-2/19/$31.00 ©2019 IEEE

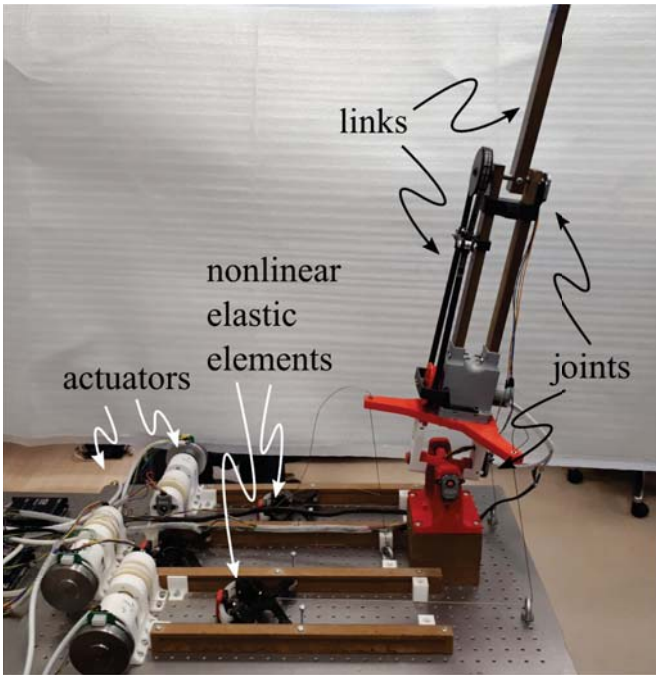

Fig. 1. Physical setup of the 3-DoF VIA robot.

at all times such that accidental collision does not cause harm. As a result, ISO10218 standard [13] introduced several requirements. At least one of these have to be satisfied to establish safe pHRI in an industrial environment. The requirements include constraint on the velocity of the Tool Center Point with upper limit of 0.25 m/s, constraint on the maximum dynamic power with upper limit of 80 W, and the constraint on the maximum static force that must be less than 150 N. However, according to [11], motion of the robot under this criteria is highly restricted and efficiency is reduced.

Augmented Reality (AR) has emerged in recent years as an innovative tool in education, entertainment and industry. AR that combines real-world with the synthetically generated information is considered as a novel tool for human-machine interaction [14]. AR techniques were utilized for engineering applications, such as repair, maintenance, assembly, and motion planning [14], [15]. In "Building Information Modeling" application, AR was used to establish an efficient mechanism for management of information via 3D visualization [16]. Authors state that further integration of AR tools into the manufacturing will advance information sharing and communication. An extensive use of AR in service works for various production-based industries, such as automobile, aerospace, power and processing plants, was described in [17]. AR was integrated into manufacturing planning in [18]. This allows humans to work within enhanced manufacturing environment, by improving processes of control and maintenance. An AR application capable to achieve real-time monitoring and collision detection based on the sensory data was introduced in [12], where velocity constraint of the system was defined based on the the data collected from the depth cameras.

In this work, we present an AR-based framework for the visualization of safe/danger zones in the workspace of a robot. This method allows human operator to see the potential danger zones in robot's workspace. Based on this information (i.e. cognizant of the danger zones), an operator can make correct decisions and move safely around the robot. The rest of the paper is organized as follows: Section II recaps different methodologies to evaluate the potential danger level, which is followed by our safety aura visualization method in Sec. III. Our case study and results are presented in Sec. IV. The paper is concluded in Sec. V.

II. Background

A. Danger-Indexes

The critical impact forces and stresses were utilized as the danger evaluation measures by Ikuta et al. [19]. Danger-indexes for the robot were generated based on several factors. Firstly, the distance l between a human and a robot with mass m was considered. Given the approaching velocity v and the constant deceleration a of the robot link prior to the impact, the distance l affects the velocity of the impact. The arising impact force is

$$F = m\frac{\sqrt{v^2 - 2la} - v'}{\Delta t}, \tag{1}$$

where Δt is the duration of the impact and v' is the link velocity after the impact. The impact force is affected by the posture of the robot. Moment of inertia and joint stiffnesses come into play in this case. Combining all of the factors, the danger-index α is calculated as the ratio $\alpha = F/F_c$, where F_c is the critical impact force. Based on these factors, the authors developed the "danger-index chart" that indicates the value of the danger-index for a robot from all possible directions on a horizontal plane. Danger-indexes enable the assessment of the contribution of each safety strategy to the overall safety performance of the robot. When the overall danger-index $\alpha_{all} > 1$, then the robot might injure a human. The objective of the safety design and control is to make α_{all} as small as possible.

The method of Ikuta et al. has some shortcomings for danger evaluation in pHRI. Since the impact force was taken as an evaluation measure, the danger-indexes based on the distance and velocity had to be expressed indirectly through the impact forces. At this stage several assumptions were introduced, which restrict the generality of the method. For example, an impact was assumed to result in a constant deceleration of a robot link. Another shortcoming is that the "danger-index chart" displays the danger zones only in the horizontal 2-D plane. A method capable of visualizing the danger zones in 3D space would be necessary for real-world applications. Also, the method can be classified as being more reactive than proactive. Thus, it is capable to indicate the current value of the safety and potential danger, however, does not allow to foresee the evolution of the danger with time.

B. Head Injury Criteria (HIC)

HIC is used to predict the skull fracture and brain injury, and is widely utilized for assessing the injury risks in automotive industry [9]. Relationship of HIC to the injury risks is derived from the analysis of simple mass-spring-mass model of the impact [9]. HIC is calculated from the measurements of the forces and accelerations experienced by the crash test dummies. The formula of HIC is given as

$$HIC(\Delta t_{max}) = max_{t1,t2}[(\frac{1}{\Delta t}\int_{t_1}^{t_2} a^*(t)\,dt)^{2.5}\Delta t], \quad (2)$$

where $\Delta t = t_2 - t_1$ and $\Delta t \leq \Delta t_{max}$, $a^*(t)$ stands for the normalized head acceleration expressed in $g = 9.8$ m/s^2, and t stands for time measured in seconds. As the normalized head acceleration is unitless, the HIC is expressed in units of seconds. Conventionally, HIC values higher than 1000 are considered as dangerous. HIC by itself cannot be used to evaluate the injury, therefore, is it linked to the Abbreviated Injury Scale (AIS) [11]. AIS measures the injury levels and scales them between zero (no injury) and six (fatal).

According to HIC, a massive robot moving with the speed less than 2 m/s will not cause severe danger [9]. However, in the case of head clamping, a robot moving with moderate speeds can severely injure a human [11]. Robots for pHRI operate at much slower speeds than the ones considered in automotive crash tests. Therefore, even though the HIC threshold of the safety limit is not crossed during the robot collision, a human subject can still be injured due to high impact forces [11]. As a result, danger evaluation criteria based on the moment of inertia and head acceleration after the collision, such as HIC, is not suitable for defining the safety limits in pHRI.

C. Gadd Severity Index (GSI)

GSI [10], expressed as an exponential weighting factor, is another metric for the evaluation of head and brain injuries. Due to the exponential weighting, as the intensity of the pulse (e.g. force, acceleration, pressure, stress or strain) slightly increases, the injury threshold increases substantially. GSI can be expressed as

$$I = \int (a(t))^n\,dt, \quad (3)$$

where $a(t)$ represents the acceleration, force, or pressure of the response function producing the threshold of injury and $n > 1$ is the weighting factor.

Zhang et al. [20] studied mid-traumatic brain injuries using recordings of the head-to-head collisions occurred during professional football games. Haddadin et al. [11] pointed out that despite being a popular metric for comparing the relative severity of pulses, effectiveness of GSI in pHRI that involve low speeds and inertias is not yet justified. GSI was developed based on the data with high velocities and inertias.

III. Distance and Velocity-Based Safety-Index

Simple human errors such as lack of attention or training cause most of the accidents in pHRI. In order to decrease the number of accidents, the International Organization for Standardization (ISO) introduced a framework which deals with risk management, probability assessment of the injury and development of accident avoidance measures. However, this framework does not leverage the potential of visualization techniques to increase the human awareness of the danger. Accidents can be decreased if a human would possess visual knowledge about the robot workspace. This would be more useful if the danger zones can be visualized in 3D-space. Additionally, it would be advantageous to have a danger evaluation method, which only considers kinematic properties of a robot and is independent from the explicit relative location of a human with respect to a robot.

Ikuta et al. [19] suggested that the danger-index should include measurements, such as the distance between the robot and the user, their relative velocity, as well as inertia and stiffness characteristics of the robot. However, they used only the measurements related to the end-effector for danger evaluation. Even though the end-effector has the highest velocity for serial manipulators, any part of a robot can collide with a human in reality.

Our method increases human awareness of the risks by providing visual cues about the potential danger in the robot's workspace for each task. Specifically, we evaluate qualitatively the collision danger in various regions of robot's workspace. We then convey this information using an appropriate visualization. Our danger evaluation algorithm uses the distance and velocity information of the robot. As a result, we create a safety aura around the robot, where different regions are assigned with specific colors.

In the case of a severe collision with a robot, a human suffers mostly due to mechanical injuries. Severity of the mechanical injury depends on the magnitude and duration of the impact force and stress. Impact force depends on the relative collision velocity between the robot and the human. It also depends on the inertial properties of the robot links, surface properties of the robot and the posture of the human at the instant of collision. However, these factors are hard to measure. Therefore, we utilized easy-to-measure distance and velocity metrics to evaluate the danger-index. Instead of utilizing danger-index to evaluate the level of danger, we can estimate safety by using safety-index. Danger-index and safety-index are inversely correlated, i.e. higher danger-index means lower safety-index and vice versa.

There are two main components in our safety-index evaluation method: 1) distance factor and 2) velocity factor. Let us consider a VIA robot at an arbitrary moment in time (see Fig. 2). A point p_k is randomly chosen from the reachable workspace of this robot. Then multiple points are chosen on the robot, such that each link contributes two points (the midpoint and the distal end of the link). Radius vectors from these points to the point p_k are denoted as $\mathbf{r_i}$, $i = 1, .., 2n_l$, where n_l is the number of robot links. We assume that the trajectory consisting of n_t uniformly sampled points for the VIA robot is given. The robot configuration (e.g. joint angles or end-effector pose) at discrete times $t_j, j = 1, .., n_t$ can be obtained using this trajectory information.

The average distance between the point p_k and the VIA robot at time t_j is $d_j^k = \frac{1}{2n_l}\sum_{i=1}^{2n_l}||\mathbf{r}_i||$, where the operator $||\cdot||$ denotes the Euclidean norm. The distance safety factor d_k^{safe} is found by evaluating the average value of the d_j^k for all configurations along a trajectory as

$$d_k^{safe} = \frac{1}{n_t}\sum_{j=1}^{n_t} d_j^k. \quad (4)$$

In essence, d_k^{safe} provides the distance from the point p_k to the robot averaged over all links and the whole trajectory.

The same workspace points p_k are utilized to estimate the velocity safety factor v_k^{safe}. Given the translational velocities of the link points $\mathbf{v_i}, i = 1,..,2n_l$ (see Fig. 2), we can estimate the velocity components along $\mathbf{r_i}$ as $\mathbf{v_i}\cdot\mathbf{r_i}$. The average velocity component of the robot links directed toward the point p_k at time t_j is $v_j^k = \frac{1}{2n_l}\sum_{i=1}^{2n_l}\mathbf{v_i}\cdot\frac{\mathbf{r_i}}{||\mathbf{r}_i||}$. The

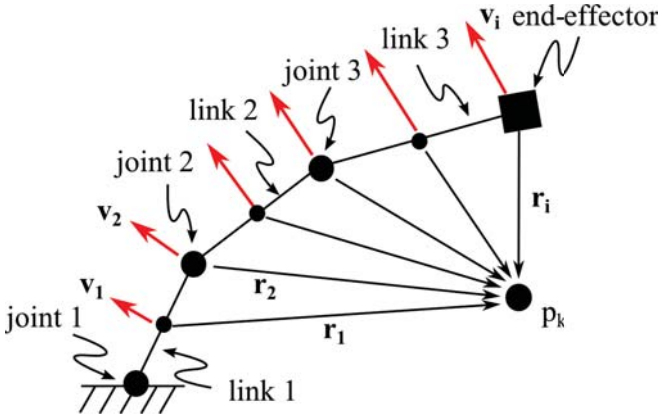

Fig. 2. Schematics of a robot and its workspace used for danger evaluation.

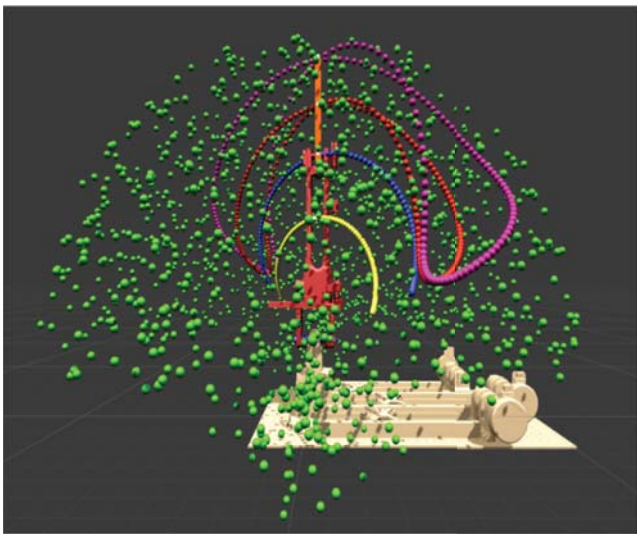

Fig. 3. Visualization of workspace and trajectory points for the VIA robot.

velocity safety factor is then calculated as

$$v_k^{safe} = \frac{1}{n_t}\sum_{j=1}^{n_t} v_j^k. \quad (5)$$

Similar to d_k^{safe}, v_k^{safe} estimates the velocity of the links directed toward the point p_k averaged over all links and the whole trajectory. This procedure is repeated for n_p visualization points in the workspace $p_k, k = 1,..,n_p$. As a result, there are n_p values of d_k^{safe} and v_k^{safe}.

$d_k^{safe} \in [0,\infty)$ and $v_k^{safe} \in (-\infty,\infty)$ describe roughly how far a robot is from the point p_k and whether it is moving towards or away from that point. As the d_k^{safe} becomes larger and the v_k^{safe} becomes smaller, the safety of the point p_k with respect to the collision increases. Our aim is to use these factors for safety aura visualization. Therefore, they need to be scaled to match a color coding. If the minimum safe distance and maximum safe velocity values are correspondingly denoted as d^{danger} and v^{danger}, then safety parameters are scaled as $d_k^{*safe} = d_k^{safe}/d^{danger}$ and $v_k^{*safe} = v_k^{safe}/v^{danger}$. If $d_k^{safe} > d^{danger}$, then $d_k^{*safe} \triangleq 1$. The safety-index SI_k^a of the point p_k can be expressed as

$$SI_k^a = \alpha d_k^{*safe} + (1-\alpha)\frac{1}{v_k^{*safe}}, \quad (6)$$

where $\alpha \in [0,1]$ is the weighting coefficient. If $v_k^{safe} > v^{danger}$, then we define $1/v_k^{*safe} \triangleq 0$, while if $v_k^{safe} < 0$ then $1/v_k^{*safe} \triangleq 1$. As a result, the following inequalities are satisfied always $0 \le d_k^{*safe} \le 1$ and $0 \le 1/v_k^{*safe} \le 1$. Finally, the point is dangerous if $SI_k^a = 0$, while the point is safe if $SI_k^a = 1$.

Due to double averaging operator employed in the above method, it does not provide accurate description of the workspace safety of the robot. In other words, averaging method smooths and filters the high and low values of safety factors. As a result, the calculated safety-index does not show the exact danger zones. In order to devise a more accurate method, we employed the minimum value for distance and maximum value for velocity for a given point p_k. In other words, $d_j^k = \min\{||\mathbf{r}_i|| : i = 1,..,2n_l\}$ and $d_k^{safe} = \min\{d_j^k : j = 1,..,n_t\}$, and $v_j^k = \max\{\mathbf{v_i}\cdot\frac{\mathbf{r_i}}{||\mathbf{r}_i||} : i = 1,..,2n_l\}$ and $v_k^{safe} = \max\{v_j^k : j = 1,..,n_t\}$. After scaling, the safety-index is found as before $SI_k^m = \alpha d_k^{*safe} + (1-\alpha)/v_k^{*safe}$. Finally, the safety aura around the workspace of the robot can be visualized by color-rendering the numerical values of the SI_k^a and/or SI_k^m at points p_k.

IV. Case Study

The virtual model of the VIA robot manipulator with two links was utilized in the simulations. The lower link was connected to the fixed base via a universal joint, while the upper link was connected to the lower link by a revolute joint. The virtual model also included three brushless actuators, nonlinear elastic elements (NEE) and linear guides for the smooth motion of NEEs. Overall, the link side of the VIA

robot has three DoF and is represented by three angles. Trajectory for the VIA robot manipulator was generated by imposing sinusoidal functions for three angular positions. The generated trajectory had $n_t = 100$ time points and at each time point coordinates of the $2n_l = 4$ points (two points for each link) were recorded. Then $n_p = 1500$ points were randomly selected from the reachable workspace of the VIA robot. Based on [9], we selected $d^{danger} = 2$ m and $v^{danger} = 2$ m/s. The simulator calculated and assigned the safety-indexes SI_k^a and SI_k^m for each of the selected points.

Unity 3D game development platform was utilized as our simulation environment. The safety evaluation algorithm, as well as the colored sphere object creation within the workspace of the robot, were implemented via a C# script compiled in Visual Studio 2017. By integrating main platform with Vuforia [21], our application was able to detect the AR markers and project the virtual robot with the corresponding aura into the real-world. A workstation (Intel Xeon CPU E5-2620 v4) with Windows 10 operating system was utilized for the experiments.

Figure 3 shows the workspace of the robot with randomly chosen $n_p = 1500$ points (green). It also depicts a set of four points, which define the two links of the VIA robot (midpoints and distal ends of the links). As the robot follows the predefined trajectory with $n_t = 100$, these four points are shown in yellow, blue, red and pink colors.

To illustrate the performance of the safety aura visualization algorithm, simulations of the VIA robot motion were generated. Spheres were created and colored based on the values of the safety-index at each point p_k in the workspace of the robot. The color of each sphere is assigned according to a colormap from green to red. Specifically, the workspace points p_k with $SI_k^a = SI_k^m = 0$ (dangerous) were colored in red, while values $SI_k^a = SI_k^m = 1$ (safe) corresponded to the green color. As mentioned in Sec. III, two safety-indexes, SI_k^a and SI_k^m, were utilized for aura visualization. As expected, the safety-index SI_k^a, which is based on the averaging method, was not accurate and was showing the whole robot workspace as safe even for regions where the link velocity magnitudes were above the selected threshold value v^{danger}. On the other, hand, the safety-index SI_k^m resulted in a more refined representation of the safety. The visual representation of the safety aura based on SI_k^m is shown in the Fig. 4. SI_k^m (with $\alpha = 0.5$) is shown at the bottom row, while its distance d_k^{*safe} and velocity v_k^{*safe} components are shown at the top and middle rows, respectively. It can be noticed that the distance component correctly represents regions of the workspace, where the robot does not pass through as safe. The velocity component shows the regions of workspace, toward which the robot links move at high velocity at any point in time as dangerous, even though the robot does not reach those points. Safety-index SI_k^m shows the composite effect of distance and velocity on safety evaluation.

The generated safety aura was visualized as AR image with the assistance of Vuforia package in Unity 3D. Performance of the AR application was demonstrated via the use of a web camera (Logitech HD 720p), a computer monitor and one Vuforia marker, which were used for the AR image tracking. The overlay of the generated safety aura and the robot in the real-world is shown in the Fig. 5.

V. Conclusion and Future Works

In this work, we presented our safety aura concept, an AR-based visualization tool, to improve the safety of pHRI. At the core of our method, we explicitly evaluate the safety of the workspace points with respect to a potential collision. The safety-index takes into account the distance and velocity metrics of the VIA robot with respect to arbitrary points in the robot workspace. Our method is independent from the user, depends only on the kinematics of the VIA robot and provides the safety information in 3D. We performed simulation experiments in order to verify the feasibility of the safety-index visualization tool. Specifically, a trajectory of the two-link 3-DoF VIA robot was considered. Safe and dangerous regions of the robot workspace were identified and visualized with respect to the whole trajectory.

This AR application might be useful for reducing accidents caused by the human errors in industrial settings. Our method evaluates safety of the whole trajectory. Therefore, it can be considered as a 'static' method. In the future, we plan to extend our method such that it can show safe/danger zones in real-time (while the robot performs a motion) using a limited window of past observations and future predictions. Furthermore, our safety index can be improved by incorporating additional variables such as robot impedance or human mental and physical fatigue.

References

[1] International Federation of Robotics, "Executive summary world robotics 2017 industrial robots," https://ifr.org/free-downloads/, 2017.

[2] A. Albu-Schaeffer *et al.*, "The DLR lightweight robot: Design and control concepts for robots in human environments," *Industrial Robot*, vol. 34, no. 5, pp. 376–385, 2007.

[3] A. Calanca, R. Muradore, and P. Fiorini, "A review of algorithms for compliant control of stiff and fixed-compliance robots," *IEEE/ASME Transactions on Mechatronics*, vol. 21, no. 2, pp. 613–624, Apr 2016.

[4] S. Haddadin *et al.*, "Collision detection and reaction: A contribution to safe physical human-robot interaction," in *Proc. of the IEEE/RSJ International Conference on Intelligent Robots and Systems (IROS)*, Sep 2008, pp. 3356–3363.

[5] B. Vanderborght *et al.*, "Variable impedance actuators: A review," *Robotics and Autonomous Systems*, vol. 61, no. 12, pp. 1601 – 1614, 2013.

[6] A. Zhakatayev, M. Rubagotti, and H. A. Varol, "Closed-loop control of variable stiffness actuated robots via nonlinear model predictive control," *IEEE Access*, vol. 3, pp. 235–248, 2015.

[7] ——, "Time optimal control of variable stiffness actuated systems," *IEEE/ASME Transactions on Mechatronics*, 2017.

[8] A. Baimyshev, A. Zhakatayev, and H. A. Varol, "Augmenting variable stiffness actuation using reaction wheels," *IEEE Access*, vol. 4, pp. 4618–4628, 2016.

[9] D. Gao and C. W. Wampler, "Head injury criterion," *IEEE Robotics Automation Magazine*, vol. 16, no. 4, pp. 71–74, December 2009.

[10] C. W. Gadd, "Use of a weighted-impulse criterion for estimating injury hazard," in *SAE Technical Paper*. SAE International, 02 1966.

[11] S. Haddadin, A. Albu-Schaffer, and G. Hirzinger, "Requirements for safe robots: Measurements, analysis and new insights," *The International Journal of Robotics Research*, vol. 28, no. 11-12, pp. 1507–1527, 2009.

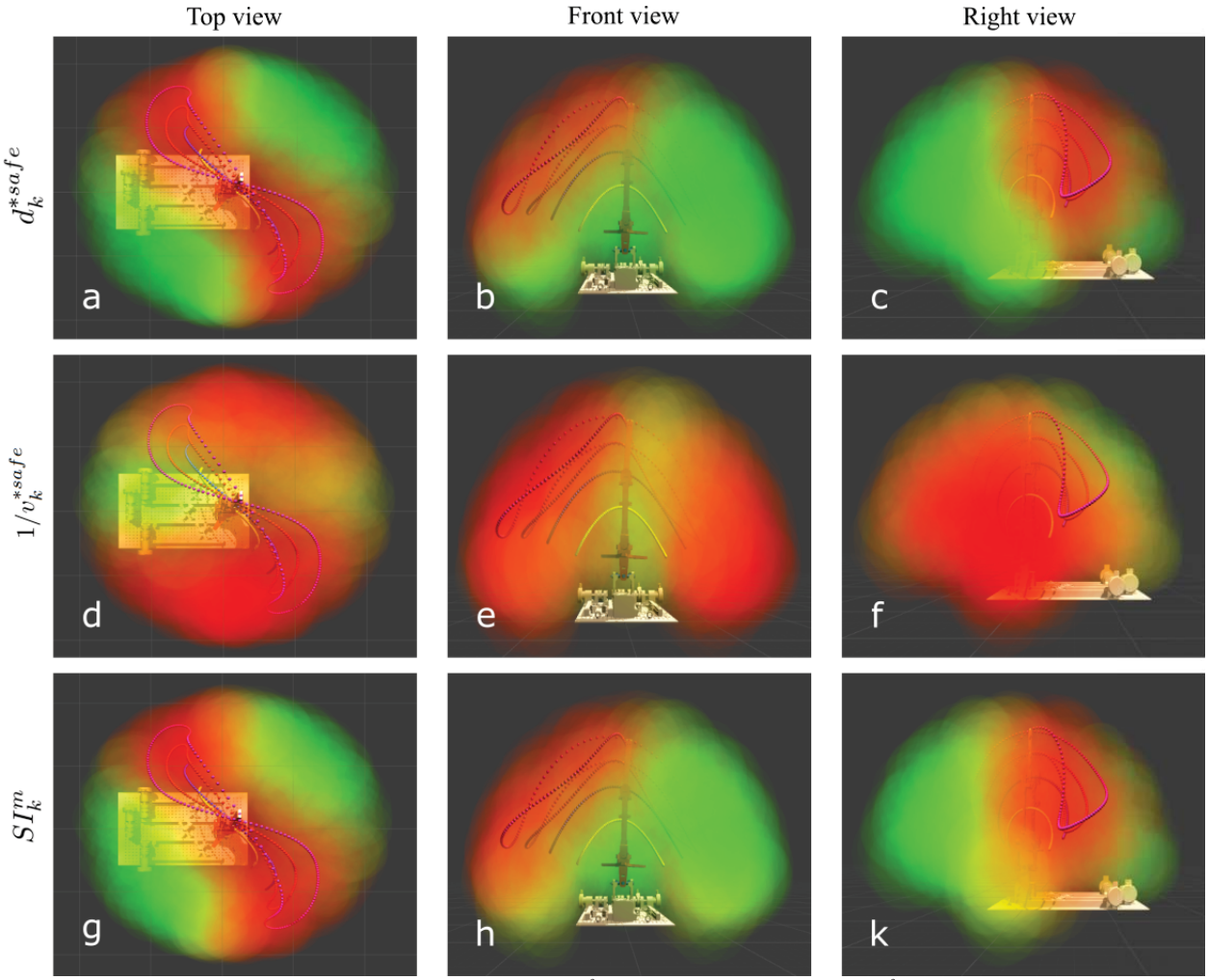

Fig. 4. Safety aura visualization for the VIA robot for distance-based d_k^{*safe} (top row), velocity-based $1/v_k^{*safe}$ (middle row), and composite safety-index SI_k^m (bottom row). Three views are considered: top (left column), front (middle column) and right (right column), $\alpha = 0.5$.

[12] E. Matsas, G.-C. Vosniakos, and D. Batras, "Prototyping proactive and adaptive techniques for human-robot collaboration in manufacturing using virtual reality," *Robotics and Computer-Integrated Manufacturing*, vol. 50, pp. 168 – 180, 2018.

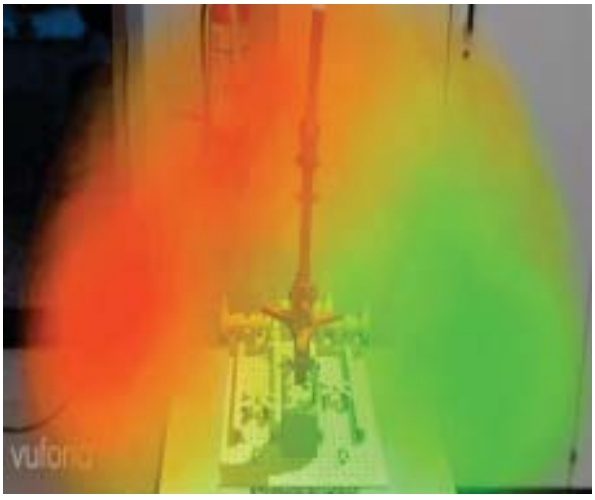

Fig. 5. Real-world safety aura using AR markers and the web camera.

[13] ISO 10218-2, *Robots and robotic devices - Safety requirements for industrial robots - Part 2: Robot systems and integration*. Geneva, Switzerland: International Organization for Standardization, Jul 2011.

[14] R. Azuma *et al.*, "Recent advances in augmented reality," *IEEE Computer Graphics and Applications*, vol. 21, no. 6, pp. 34–47, Nov 2001.

[15] D. B. Espíndola *et al.*, "A model-based approach for data integration to improve maintenance management by mixed reality," *Computers in Industry*, vol. 64, no. 4, pp. 376 – 391, 2013.

[16] X. Wang *et al.*, "Integrating augmented reality with building information modeling: Onsite construction process controlling for liquefied natural gas industry," *Automation in Construction*, vol. 40, pp. 96 – 105, 2014.

[17] W. Wohlgemuth and G. Triebfürst, "Arvika: Augmented reality for development, production and service," in *Proc. of Designing Augmented Reality Environments (DARE)*, 2000, pp. 151–152.

[18] F. Doil *et al.*, "Augmented reality for manufacturing planning," in *Proceedings of the Workshop on Virtual Environments 2003*, ser. EGVE '03. New York, NY, USA: ACM, 2003, pp. 71–76.

[19] K. Ikuta, H. Ishii, and M. Nokata, "Safety evaluation method of design and control for human-care robots," *The International Journal of Robotics Research*, vol. 22, no. 5, pp. 281–297, 2003.

[20] Z. Liying, Y. King, and K. Albert, "A proposed injury threshold for mild traumatic brain injury," *Journal of Biomechanical Engineering*, vol. 126, no. 2, pp. 226–236, 2004.

[21] S. Vuforia, "Vuforia developer portal," 2013.